

Temperature Dependence of the Spin Torque Effect in Current-Induced Domain Wall Motion

M. Laufenberg,¹ W. Bührer,¹ D. Bedau,¹ P.-E. Melchy,¹ M. Kläui,¹ L. Vila,²
G. Faini,² C. A. F. Vaz,³ J. A. C. Bland,³ and U. Rüdiger¹

¹*Fachbereich Physik, Universität Konstanz, Universitätsstraße 10, 78457 Konstanz, Germany*

²*Laboratoire de Photonique et de Nanostructures-CNRS, Route de Nozay, 91460 Marcoussis, France*

³*Cavendish Laboratory, University of Cambridge, Madingley Road, Cambridge, CB3 0HE, United Kingdom*

We present an experimental study of domain wall motion induced by current pulses as well as by conventional magnetic fields at temperatures between 2 and 300 K in a 110 nm wide and 34 nm thick $\text{Ni}_{80}\text{Fe}_{20}$ ring. We observe that, in contrast with field-induced domain wall motion, which is a thermally activated process, the critical current density for current-induced domain wall motion increases with increasing temperature, which implies a reduction of the spin torque efficiency. The effect of Joule heating due to the current pulses is measured and taken into account to obtain critical fields and current densities at constant sample temperatures. This allows for a comparison of our results with theory.

PACS numbers: 72.25.Ba, 75.60.Ch, 75.75.+a, 85.70.Kh

The interplay between spin currents and domain walls in magnetic nanostructures has been studied intensively in the last decade, driven by fundamental interest in the basic physical mechanisms involved. Furthermore, current-induced magnetization reversal by domain wall motion is a promising alternative to the conventional field-induced reversal for technological applications in nonvolatile memories and sensors, which has led to an increase in research in this field [1]. The phenomenon of current-induced domain wall motion has been long known [2,3] and recently controlled current-induced motion of single domain walls in magnetic nanostructures has been achieved. Several important aspects such as domain wall velocities [4,5], critical current densities [6–8], thermally assisted motion [9], and the deformation of the domain wall spin structure due to current [4] have been addressed. Current-induced switching has been also investigated in a trilayer pillar geometry at variable temperatures [10,11]. The underlying theory of interaction between current and magnetization is still controversial. Different approaches have been suggested in the ballistic limit [12,13] as well as in the diffusive limit [2,12]. An adiabatic spin torque has been introduced into the Landau-Lifshitz-Gilbert equation of magnetization dynamics [12,14,15]. Motivated by large discrepancies between experiment and theory, a nonadiabatic term was included [16,17]. The relative importance of the two torques in domain wall motion is still the subject of much debate [16–18]. In order to gain information on the (non-)adiabaticity of the spin torque, a study of domain wall motion as a function of current and field at a constant sample temperature is needed. Using combinations of current and field allows one to compare the theoretical calculations [18] of the dependence of the critical current on the applied field with the experimental results. Of particular importance for comparison of experiment and theory is a constant sample temperature to separate spin torque and temperature effects, because existing theory so far neglects heating effects. Since significant Joule heating due

to injected current pulses was observed [19], this effect must be quantitatively measured and taken into account. The possibility of describing spin torque as an effective field has been put forward recently [20]. In the field-induced case, domain wall motion is thermally assisted [21], but the effects of thermal activation on current-induced domain wall motion have so far only been studied theoretically and only in the limit of small excitations [22]. Thermally excited spin waves have been neglected in the 0 K theory of spin torque, but theoretically the current was shown to alter the spinwave spectrum [23,24]. Thus to understand the interplay between spin torque and thermal effects and to obtain information on the nonadiabaticity of the torque, current-, and field-induced domain wall motion experiments at different sample temperatures are needed.

In this Letter, we present results of current- and field-induced domain wall motion at cryostat temperatures between 2 and 200 K. The Joule heating of the current is explicitly measured and used to correct the data in order to compare the results for a constant sample temperature with theoretical work. The critical current density for domain wall motion increases with increasing temperature, which implies a reduction of the spin torque efficiency.

A scanning electron microscopy (SEM) image of a 34 nm thick and 110 nm wide $\text{Ni}_{80}\text{Fe}_{20}$ ring with 1 μm diameter with electrical contacts, which was fabricated on a naturally oxidized Si substrate as described in Ref. [25], is shown in Fig. 1(a). The ring geometry has the advantage that a domain wall can easily be generated and positioned by applying a homogeneous magnetic field. Domain walls in such structures are head-to-head or tail-to-tail 180° domain walls with a vortex or a transverse spin structure [26,27]. For this particular geometry, the domain wall type was determined to be a vortex wall using magnetoresistance measurements as detailed in Ref. [28]. A micromagnetic simulation performed with the OOMMF code [29] (parameters: $M_s = 800 \times 10^3$ A/m, $A = 13 \times 10^{-12}$ J/m,

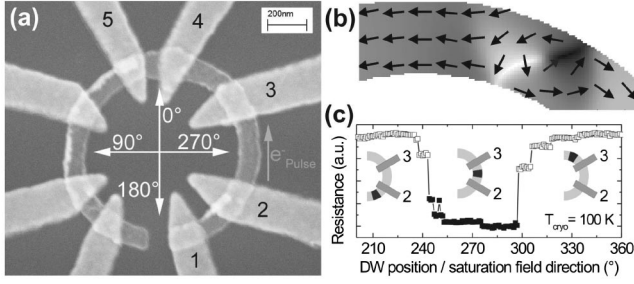


FIG. 1. (a) SEM image of the $\text{Ni}_{80}\text{Fe}_{20}$ ring investigated (34 nm thick, 110 nm wide, $1 \mu\text{m}$ diameter) with the numbered contacts and the polar angles indicated. (b) OOMMF simulation of a vortex wall in a ring with the sample geometry. (c) Resistance of the ring area between contacts 2 and 3 as a function of the wall position (schematically shown) at $T_{\text{cryo}} = 100 \text{ K}$.

3 nm cell size) and shown in Fig. 1(b) agrees with the experimentally observed vortex wall spin structure.

Magnetoresistance measurements were carried out using a standard lock-in technique in a four-point configuration. A constant ac current of typically $5 \mu\text{A}$ was applied between contacts 1 and 5 while the voltage drop was measured between contacts 2 and 3 [cf. Fig. 1(a)]. The magnetization configurations with a domain wall situated between and outside the voltage contacts, respectively, correspond to different resistance levels due to the anisotropic magnetoresistance contribution of the domain wall [30]. Reference curves, as shown in Fig. 1(c) for $T_{\text{cryo}} = 100 \text{ K}$, were taken by saturating the sample in directions between 220° and 340° [cf. Fig. 1(a)] and subsequently relaxing the field to zero and measuring the resistance [30]. These curves allow us to quickly ascertain the wall position by means of a resistance measurement. Current pulses with $10 \mu\text{s}$ duration were applied between contacts 1 and 4 generating current densities of up to $2.5 \times 10^{12} \text{ A/m}^2$ in the ring structure. In order to determine the combinations of current and field that result in domain wall motion, we have executed the following experimental sequence typically 10 times for each combination of field strength, current density, and temperature: (i) An external field is applied along 273° and released, so that a domain wall is created at this particular position. (ii) The resistance is measured. Using the reference curve mentioned before, we crosscheck that the domain wall is correctly positioned. (iii) An external magnetic field is applied perpendicularly to the direction of the saturation field along 3° (field and current parallel) or along 183° (field and current antiparallel), respectively. (iv) A current pulse is injected in addition to the field. (v) The resistance is measured again to discern whether the domain wall has moved out of the area between the voltage contacts or not. We obtain the diagrams presented in Figs. 2(a) and 2(b). The different symbols indicate the field and current values necessary for domain wall displacement at different temperatures between 2 and 200 K.

We first turn to the data presented in Fig. 2(a), where current and field are parallel. At zero current and a temperature of 2 K (black squares), a field of about 22 mT is needed to move the domain wall, which is pinned due to edge irregularities as visible in Fig. 1(a). The critical field at zero current decreases with increasing temperature as expected, since the increased thermal energy helps to overcome the energy barrier of the pinning potential. The temperature dependence of the critical field for zero current [black squares in inset of Fig. 2(a)] can be described using the model presented in Ref. [21], which indicates that thermally assisted field-induced domain wall motion is the dominant process. In the low temperature regime ($\leq 20 \text{ K}$), already small current densities $0.2 \times 10^{12} \text{ A/m}^2$ assist the depinning process and reduce the critical field [Fig. 2(a)]. We attribute this decrease predominantly to the Joule heating of the current pulses, because even small temperature increases can lead to a large decrease of the critical field as discussed above [inset of Fig. 2(a)]. An additional mechanism suggested by He *et al.* [18] is that the adiabatic torque of the current helps to displace the domain wall center away from the pinning site which allows small fields to displace it. As the current density is increased, we see no change in the critical field, until a threshold current density of 0.5 to $0.8 \times 10^{12} \text{ A/m}^2$ is reached, above which a reduction of the critical field takes place. The existence of such a threshold is in agreement with theoretical results that take into account the edge roughness of a sample [17,18]. Above this threshold, we obtain a decrease [continuous lines in Fig. 2(a)] of the critical field until the critical current density $j_c^{H=0}$ at zero field is reached at which the current moves the domain wall without any external field. When field and current act in a way as to

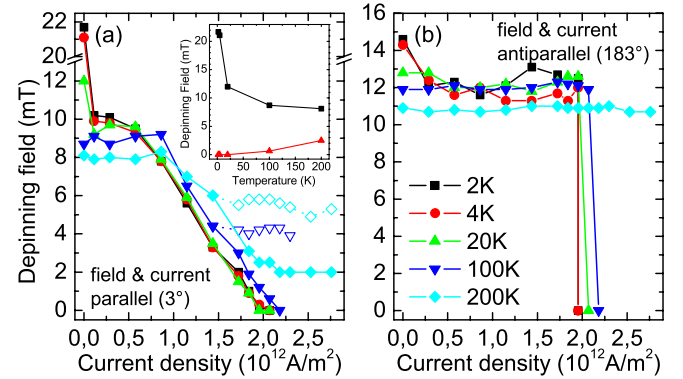


FIG. 2 (color online). Domain wall depinning at the temperatures T_{cryo} indicated in the legend for (a) current and field parallel and (b) current and field antiparallel. All lines are guides to the eye. The statistical errors of the critical fields are of the order of ± 0.5 to 1 mT . For values above the lines, the domain wall is displaced, below it remains pinned. Open symbols in (a) show the splitting of the boundary for high temperatures as explained in the text. The inset of (a) shows the critical field as function of the temperature for zero current (black squares) and for $j = 2.07 \times 10^{12} \text{ A/m}^2$ (red triangles).

move the domain wall in opposite directions, the $H_c(j)$ dependence exhibits a different behavior [Fig. 2(b)]. The decrease for very small currents (black discs and red circles for $j = 0.2 \times 10^{12}$ A/m²) can be explained by Joule heating like in Fig. 2(a). The difference in the absolute critical field reduction between the two field directions is due to the asymmetry of the pinning potential, which can be seen comparing the critical fields in Figs. 2(a) and 2(b) for zero current. Such asymmetries are always present in these samples due to geometrical irregularities, etc. [31]. For current densities above 0.2×10^{12} A/m², no significant change of the critical field can be observed up to the critical current density. This behavior is different from the results of Vernier *et al.* [6], who use continuous currents leading to a reduction of the critical field. In our case, using current pulses, we observe that the spin torque effect and the magnetic field act in opposite senses, which leads to a constant critical field. This means that Joule heating cannot be dominating in this situation.

We now turn back to the case where field and current are parallel in order to compare these results with theory. Since theoretical work is usually based on a constant sample temperature we first have to quantitatively analyze the effect of Joule heating due to the current. We have measured the sample temperature during injection as described in Ref. [19], and observed that the heating is much weaker than found therein, which might be due to different substrates used [32]. The heating depends on the cryostat temperature T_{cryo} . For low temperatures ($T_{\text{cryo}} \leq 20$ K), the sample heats up by $\Delta T \approx 100$ K at a current density of 2.1×10^{12} A/m² while for $T_{\text{cryo}} \geq 100$ K, the heating is $\Delta T \approx 60$ K [Fig. 3(a)]. This means that for all cryostat temperatures investigated, the real sample temperature T_{real} remains significantly below the Curie temperature of about 650 K. With this correction for Joule heating, we obtain the modified diagram for domain wall motion at $T_{\text{real}} = (100 \pm 5)$ K shown in Fig. 3(b). The data points are either taken at cryostat temperatures T_{cryo} so that the heating leads to a sample temperature $T_{\text{real}} = (100 \pm 5)$ K (e.g. $j = 1.88 \times 10^{12}$ A/m² injected at $T_{\text{cryo}} = 4.3$ K causes a heating of $\Delta T \approx 96$ K and therefore a sample temperature $T_{\text{real}} \approx 100$ K) or they are interpolated from measured data [33]. Only now we can meaningfully compare the experimental data with the theoretical calculations, which assume a constant temperature. For $T_{\text{real}} = 100$ K, the critical field decreases with increasing current density above a threshold of about 0.8×10^{12} A/m² [Fig. 3(b)]. This is in qualitative accordance with results of numerical calculations of the domain wall depinning from an artificial pinning site in a Ni₈₀Fe₂₀ wire at $T = 0$ K [18]. A quantitative comparison is not possible since our geometry is different. The critical current density and the shape of the $j_c(H)$ curve (Fig. 2 in Ref. [18]) crucially depend on the nonadiabaticity parameter ξ (represented by β in Ref. [17]) [18]. Fitting of the experimental data using micromagnetic simulations of our geometry can then pro-

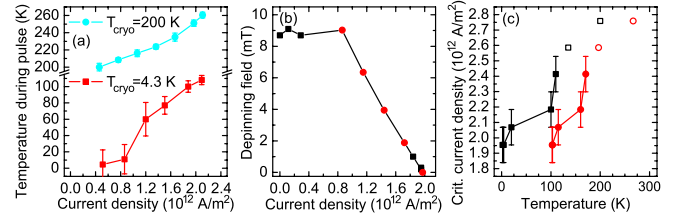


FIG. 3 (color online). (a) Temperature increase due to Joule heating as a function of current density for $T_{\text{cryo}} = 4$ K (red squares) and 200 K (blue circles). (b) Domain wall depinning for a sample temperature of 100 ± 5 K with current and field parallel. Black squares indicate measured values, red circles are interpolated. (c) Critical current density as function of the temperature. Black squares refer to the cryostat temperature T_{cryo} , red circles to real temperatures T_{real} corrected for the effect of Joule heating. Open symbols indicate maximum values of the current density injected during the sample lifetime and are therefore lower limits for the critical current density.

vide quantitative information on ξ and therefore allow us to test the available theory and to gain insight into the relative importance of the adiabatic and nonadiabatic spin torque terms.

When the critical current density is reached, the domain wall is moved without the presence of any external magnetic field. Surprisingly, this critical current density $j_c^{H=0}$ increases with increasing temperature as shown in Fig. 3(c). This is a behavior exactly opposite to field-induced motion, where the dependence of the critical field on the temperature indicates a thermally activated motion [21]. Opposite behaviors for the field and the current needed for domain wall motion as a function of temperature are observed as shown in the inset of Fig. 2(a), which indicate that thermally activated motion is dominating in the field-driven, but not in the current-driven case. To our knowledge, only Tatara *et al.* have so far included thermal effects in the theoretical description of current-driven domain wall motion [22], and they do not predict an increase of the critical current density. Temperature dependent measurements of the critical current density for switching in trilayer pillar elements [11] show a decrease with increasing temperature, which is explained in the framework of a model of spin accumulation at the interfaces. This model is obviously not applicable in our case, which is corroborated by our observation of the opposite behavior. This leads us to conclude that here a mechanism must exist which reduces the efficiency of the spin torque at increased temperature and which is dominating over thermal activation processes for the investigated geometry. Spin wave generation can be such a mechanism [12] if a symmetry breaking between magnon excitation and annihilation for different directions occurs due to the current flow. When taking into account spin currents, it was theoretically predicted [23,24] that the spin wave dispersion $\omega(\mathbf{k})$ becomes asymmetric. Because of this asymmetry, also the magnon density of states becomes asymmetric with respect to \mathbf{k} so

that for nonzero temperature the number of thermally excited spin waves becomes asymmetric as well in the presence of a current. With increasing temperature, the number of thermally excited magnons increases as well as the difference between the number of magnons with opposite wave vectors so that more angular momentum is effectively carried away and the current-induced domain wall motion becomes less efficient. For the discussion of other possible origins besides asymmetric thermally excited spin waves we consider the temperature dependence of the nonadiabaticity parameter $\xi = \lambda_{\text{exchange}}^2 / \lambda_{\text{spin flip}}^2$ [16,17]. However, a decreasing spin flip length $\lambda_{\text{spin flip}}$ with increasing temperature leads to an increase rather than a decrease of the spin torque efficiency. The exchange length $\lambda_{\text{exchange}}$ is expected to be only weakly dependent on temperature, so that $\lambda_{\text{spin flip}}$ dominates the temperature dependence of ξ . Different effects might exist that can reduce the spin torque efficiency, but we can exclude heating effects, because we have separated the influence of heating. Thermal activation as found in the field-induced case can be excluded as the dominating effect due to its opposite temperature dependence. Therefore, possible explanations for the increase of the critical current density with temperature are reduced to the effective dependence of the spin torque efficiency on temperature.

Furthermore, Fig. 2(a) shows that the curves for $T_{\text{cryo}} \geq 100$ K split at a certain current density into two branches. Experimentally, we have observed that a motion occurs for a low field, not for intermediate fields, and again for higher fields at a given current density. We interpret these two branches as the result of two different processes. Either the domain wall is moved by current and field (lower branch) or the current modifies the spin structure of the domain wall such that the critical field is increased (higher branch). The domain wall with the modified spin structure is not moved anymore by the current densities used, but only by an appropriately high magnetic field. This explains why the upper branches do not show any dependence on the current density. It was already observed experimentally [4] as well as investigated theoretically [17] that current pulses can change the spin structure of domain walls which leads to an immobilization [4]. The splitting into branches is not observed for all temperatures because the energy barriers involved in the wall spin structure transformations are temperature dependent.

In conclusion, we have systematically determined the combinations of critical fields and critical current densities necessary to move a vortex domain wall in our sample at real constant sample temperatures. This data agrees qualitatively with available theoretical calculations for a different geometry. Furthermore, we have observed a significant increase of the critical current density with temperature which is in contrast to the decrease of the critical field in the field-driven case. This indicates that the current-driven domain wall motion is not predominantly a thermally

activated process like the field-driven motion. We can thus conclude that the intrinsic spin torque efficiency is reduced with increasing temperature, which might be, for example, due to thermally excited spin waves.

The authors acknowledge support by the DFG through SFB 513, the EPSRC (U.K.), the “Région Ile de France”, and the “Conseil Général de l’Essonne”. Technical support by E. Cambriil is gratefully acknowledged.

*Electronic address: mathias.klaui@uni-konstanz.de

- [1] S. S. P. Parkin, U.S. patent No. 6 834 005 and patent application No. 10/984 055 2004.
- [2] J. C. Slonczewski, *J. Magn. Magn. Mater.* **159**, L1 (1996).
- [3] L. Berger, *J. Appl. Phys.* **55**, 1954 (1984).
- [4] M. Kläui *et al.*, *Phys. Rev. Lett.* **95**, 026601 (2005); M. Kläui *et al.* *Appl. Phys. Lett.* **88**, 232507 (2006).
- [5] A. Yamaguchi *et al.*, *Phys. Rev. Lett.* **92**, 077205 (2004).
- [6] N. Vernier *et al.*, *Europhys. Lett.* **65**, 526 (2004).
- [7] M. Kläui *et al.*, *Phys. Rev. Lett.* **94**, 106601 (2005).
- [8] J. Grollier *et al.*, *Appl. Phys. Lett.* **83**, 509 (2003).
- [9] D. Ravelosona *et al.*, *Phys. Rev. Lett.* **95**, 117203 (2005).
- [10] E. B. Myers *et al.*, *Phys. Rev. Lett.* **89**, 196801 (2002).
- [11] M. Tsoi *et al.*, *Phys. Rev. B* **69**, 100406(R) (2004).
- [12] G. Tatara and H. Kohno, *Phys. Rev. Lett.* **92**, 086601 (2004).
- [13] V. A. Gopar *et al.*, *Phys. Rev. B* **69**, 014426 (2004).
- [14] A. Thiaville, Y. Nakatani, J. Miltat, and N. Vernier, *J. Appl. Phys.* **95**, 7049 (2004).
- [15] Z. Li and S. Zhang, *Phys. Rev. Lett.* **92**, 207203 (2004).
- [16] S. Zhang and Z. Li, *Phys. Rev. Lett.* **93**, 127204 (2004).
- [17] A. Thiaville, Y. Nakatani, J. Miltat, and Y. Suzuki, *Europhys. Lett.* **69**, 990 (2005).
- [18] J. He, Z. Li, and S. Zhang, *J. Appl. Phys.* **98**, 016108 (2005).
- [19] A. Yamaguchi *et al.*, *Appl. Phys. Lett.* **86**, 012511 (2005).
- [20] J. Ohe and B. Kramer, *Phys. Rev. Lett.* **96**, 027204 (2006).
- [21] A. Himeno *et al.*, *J. Magn. Magn. Mater.* **286**, 167 (2005).
- [22] G. Tatara, N. Vernier, and J. Ferré, *Appl. Phys. Lett.* **86**, 252509 (2005).
- [23] Y. B. Bazaliy, B. A. Jones, and S.-C. Zhang, *Phys. Rev. B* **57**, R3213 (1998).
- [24] J. Fernández-Rossier *et al.*, *Phys. Rev. B* **69**, 174412 (2004).
- [25] M. Kläui *et al.*, *Appl. Phys. Lett.* **81**, 108 (2002).
- [26] R. D. McMichael and M. J. Donahue, *IEEE Trans. Magn.* **33**, 4167 (1997).
- [27] M. Laufenberg *et al.*, *Appl. Phys. Lett.* **88**, 052507 (2006).
- [28] M. Kläui *et al.*, *Physica B (Amsterdam)* **343**, 343 (2004).
- [29] OOMMF is available at <http://math.nist.gov/oommf>.
- [30] M. Kläui *et al.*, *Phys. Rev. Lett.* **90**, 097202 (2003).
- [31] M. Kläui *et al.*, *Appl. Phys. Lett.* **84**, 951 (2004).
- [32] A. Yamaguchi *et al.*, *Jpn. J. Appl. Phys.* **45**, 3850 (2006).
- [33] Since measurements for $T_{\text{real}} = 100$ K are not available for all current densities, some values have been interpolated from measurements that yield values of T_{real} just above and just below 100 K.